Design and Rapid Prototyping of Packaging Liner for Rosewood Craft based on Gyroid Infill Structure

Chen Wang,[a,b,*] Jingyao Li,[a] Tianyi Wang,[a] Qin Chu,[a] and Shuqin Wen [b]

A gyroid structure is a commonly used energy-absorbing infill structure for packaging that can be prepared by fused deposition modeling (FDM) 3D printing. In this paper, square specimens based on gyroid infill structure were designed, and the energy-absorbing performances of the square specimens were analysed by quasi-static compression testing under different printing parameters (layer height, extrusion rate, and extrusion temperature). A gourd ornament carved from rosewood was selected as the design object, and a packaging liner that highly fits the curved shape of the gourd ornament was designed through the process of reverse scanning and forward modelling. The prototype of the packaging liner was fabricated by using FDM 3D printing technology and thermoplastic polyurethane (TPU) filament. With decreased layer height, the energy absorption (E_A) value of the gyroid infill structure increased, while the specific energy absorption (S_{EA}) value first increased and then decreased. With the increased extrusion rate, the E_A value of the gyroid infill structure increased, and the S_{EA} value increased. With increased extrusion temperature, the E_A and S_{EA} values of the gyroid infill structure increased. The packaging liner developed based on the gyroid infill structure and the optimised printing parameters exhibited strong energy-absorbing performance.

DOI: 10.15376/biores.20.1.842-851

Keywords: Gyroid infill structure; Rosewood craft; Packaging liner; Rapid prototyping

*Contact information: a: College of Furnishings and Industrial Design, Nanjing Forestry University, Nanjing 210037, China; b: Jiangsu Co-Innovation Center of Efficient Processing and Utilization of Forest Resources, Jiangsu, China; *Corresponding author: 996869559@qq.com*

INTRODUCTION

Rosewood is a traditional Chinese valuable furniture material, mostly produced in tropical areas, due to slow growth, hard material, belonging to the scarce and high-quality biological resources (Huang *et al*. 2022). Rosewood craft is the creation of wood carving with rosewood as the carrier. It is also the most valuable category of wood carving craft. Its fine workmanship and novel design have inherited the essence of traditional Chinese culture (Ding *et al*. 2022). It has a strong cultural heritage and high artistic value. It is widely used as decoration in the home environment.

Because the rosewood material is expensive, and the rosewood craft has a certain artistic value, so its packaging needs to have a strong protective performance in order to reduce the damage to the rosewood craft in the logistics transport process by external force (Deng *et al*. 2023). Usually the outer packaging of the goods in the logistics transport process will be subjected to warehouse stacking, so in the design of rosewood craft packaging, it is necessary to consider the packaging structure of the energy-absorbing effect under compression conditions (Feng *et al*. 2022). The gyroid structure absorbs

energy. It is commonly prepared as an infill structure by means of fused deposition modeling (FDM) 3D printing. The application of gyroid infill structure to 3D-printed packaging liner for rosewood craft is a new attempt, which can provide effective protection for rosewood craft (Han *et al*. 2022).

In this work, a square specimen based on the gyroid infill structure was designed. The energy-absorbing performance of the square specimen was analysed by quasi-static compression testing with different printing parameters (layer height, extrusion rate and extrusion temperature). The optimised printing parameters of the gyroid infill structure were summarised. The gourd ornament carved from rosewood was selected as the design object, and the packaging liner that highly fits the curved shape of the gourd ornament was designed through the process of reverse scanning and forward modelling. Finally, a prototype of the packaging liner was fabricated by FDM 3D printing using thermoplastic polyurethane (TPU) filament. The 3D-printed packaging liner developed based on the gyroid infill structure and optimised printing parameters has strong energy-absorbing performance, which provides guidance for the customised development of energy-absorbing packaging liners for other rosewood crafts.

EXPERIMENTAL

Materials

Thermoplastic polyurethane (TPU) filament with a diameter of 1.75 mm and a Shore hardness of 90 (white, Anycubic, Shenzhen, China) was used for rapid prototyping by the fused deposition modeling method.

The TPU filament used in this study was a polyether-based thermoplastic with polytetrahydrofuran ether (PTMO) in the soft segment part, 4,4-dibenzoyl diisocyanate (4,4-MDI) in the hard segment part, and 1,4-butanediol (1,4-BDO) as the chain extender, with a glass transition temperature of about 80 °C (Chen *et al*. 2022).

Gyroid Infill Structure

The gyroid structure is a triply periodic minimal surface (TPMS). It consists of wavy curves in the plane, and in three dimensions it superimposes wavy curves into surfaces in the form of spirals, which gives the gyroid structure a triple rotational symmetry (shown in Fig. 1). The unique minimal surface configuration of the gyroid structure results in a large porosity, which absorbs a large amount of energy during deformation under pressure (Li *et al*. 2020).

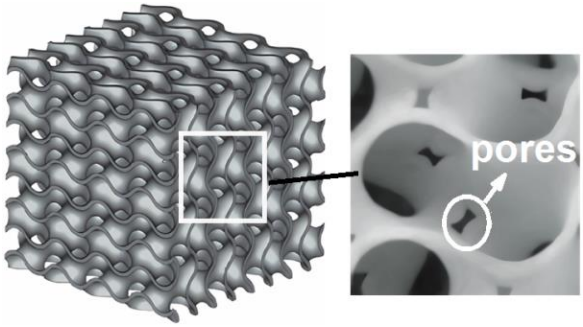

Fig. 1. Gyroid infill structure

Gyroid structure is also a commonly used infill structure for FDM 3D printing, and the print quality of the gyroid infill structure is mainly affected by the infill density (Li *et al*. 2022). With the increase of infill density, the extrusion head has more rapid deflection and consequent increase of vibration during the actual printing process, which leads to the increase of pores on the adhesive interface of adjacent layers in the gyroid structure (shown in Fig. 1). Therefore, a low density infill mode (10 to 20%) is required to print the gyroid structure, which reduces the pores in the structure and improves the print quality (Liu *et al*. 2021).

Quasi-static Compression Testing

To investigate the quasi-static compression performance of gyroid infill structure, a square specimen (size:50 mm×50 mm×50 mm) based on gyroid infill structure was designed using Solidworks software (Dassault Systemes, Education Version 2016, Paris, France). Using Cura software (Ultimaker, Cura 4.2.0, Utrecht, Netherlands) for slicing, the layer height of the square specimen was set to 0.1 mm, the extrusion rate was set to 110%, the extrusion temperature was set to 230 °C, the printing speed was set to 50 mm/s, and the infill density was set to 10% (the gyroid structure with this infill density has a lower porosity, and at the same time it can also meet the requirements of lightweighting, which saves the printing material). Finally, the TPU filament was applied and the square specimen was fabricated by FDM 3D printer (X-Y-Z printing, 0.4 mm nozzle diameter, Anycubic, Shenzhen, China). In order to improve the adhesion of the specimen to the heated bed plate, the temperature of the heated bed plate was set to 70 °C.

The quasi-static compression pre-test of the energy-absorbing performance of the square specimen was carried out using a universal mechanical testing machine (AG-X, 20kN, Shimadzu, Kyoto, Japan). The test was conducted at room temperature of 20 °C, the compression loading rate was 2 mm/min, and the quasi-static compression curves obtained from the pre-test are shown in Fig. 2. The compressive stress-strain curve of the square specimen can be divided into three zones, including the elastic deformation zone, the platform zone and the densification zone (Liu *et al*. 2020). In the elastic deformation zone, with the increase of strain, the stress shows a linear increase; in the platform zone, with the increase of strain, the change of stress is relatively smooth; in the densification zone, with the increase of strain, the stress shows a rapid increase in characteristics (Mo *et al*. 2022).

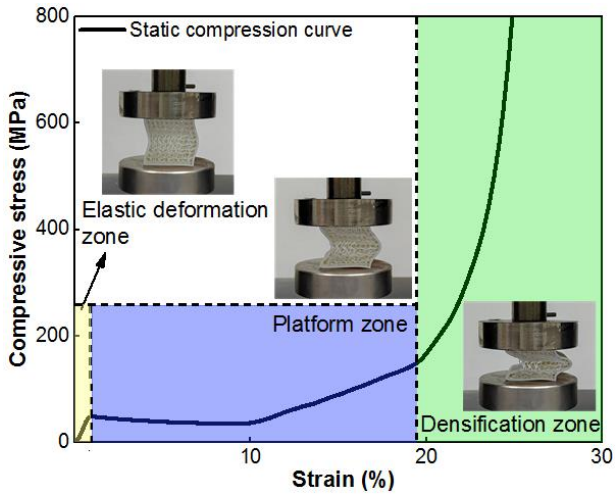

Fig. 2. Effect of triangular mesh processing

To clarify the effects of printing parameters (layer height, extrusion rate, and extrusion temperature) on the energy absorption performance of gyroid infill structure, the square specimens corresponding to each set of parameters were printed separately by FDM 3D printer. Two indicators, energy absorption (E_A) and specific energy absorption (S_{EA}), were introduced. The energy absorption (E_A) is mainly used to evaluate the sum of energy absorbed by the gyroid infill structure during plastic compression, $E_A = \int_0^{\varepsilon} \sigma(\varepsilon) d\varepsilon$, in the formula, E_A is the energy absorption (J), σ is the compressive stress (MPa), and ε is the compressive strain; the specific energy absorption (S_{EA}) indicates the absorption of energy per unit mass, $S_{EA} = \frac{E_A}{M}$, in the formula, where M is the mass of the specimen (g).

RESULTS AND DISCUSSION

Effect of Layer Height on the Energy Absorption Performance of Gyroid Infill Structure

The compression energy absorption performance of three groups of gyroid infill specimens (three of each group) at 0.1, 0.2, and 0.3 mm layer heights is shown in Fig. 3. With the decrease of layer height, the E_A value of the specimens increased, while the S_{EA} value first increased and then decreased. As the layer height decreased, the extrusion pressure from the extrusion head of the adjacent layer filaments increased, and the squeezing effect increased the bonding area of the adjacent layer filaments, which contributes to the increase of the interlayer bonding strength of the adjacent layer filaments (Yu *et al*. 2023). In the compression process, the relative slip of adjacent layer filaments due to shear force is the main cause of damage to the specimen (Qi *et al*. 2023). As the reduction of layer height leads to the increase of the interlayer bonding strength of the specimen, its overall structure is less prone to be damaged when compressed, and therefore the E_A value is larger. However, the reduction of layer height also led to an increase in the mass of the specimen, which affected the S_{EA} value (Zhu *et al*. 2020). Although the E_A value of 0.2 mm layer height was not the largest, it had a relatively small mass increase and the largest S_{EA} value compared to the 0.1 mm layer height. So 0.2 mm was the optimised layer height to improve the energy absorption performance of gyroid infill structure.

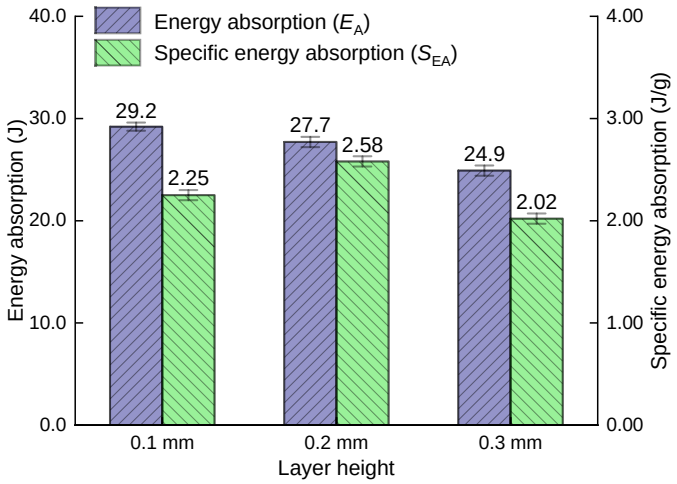

Fig. 3. Effect of layer height on the energy absorption performance of gyroid infill structure

Effect of Extrusion Rate on the Energy Absorption Performance of Gyroid Infill Structure

The compression energy absorption performance of three groups of gyroid infill specimens (three of each group) at 90, 100, and 110% extrusion rates is shown in Fig. 4. With the increase of extrusion rate, the E_A value of the specimens increased, and the S_{EA} value increased. As the extrusion rate increased, the flow rate of the molten filament extruded from the extrusion head increased slightly, and the molten filament produced flow under surface tension, filling the pores between adjacent layers (Wang *et al*. 2022). These pores are the weak points of the overall structure when the specimen is compressed. These conditions easily can result in stress concentration and lead to the destruction of the specimen (Yu *et al*. 2024). As the extrusion rate increases, the specimen porosity becomes smaller, there are fewer weak points in the structure, and the E_A value increases. The increase in extrusion rate had a small effect on the overall mass of the specimen. As the E_A value of the specimen increased, its S_{EA} value increased as well, so 110% was found to be the optimised extrusion rate to improve the energy absorption performance of the gyroid infill structure.

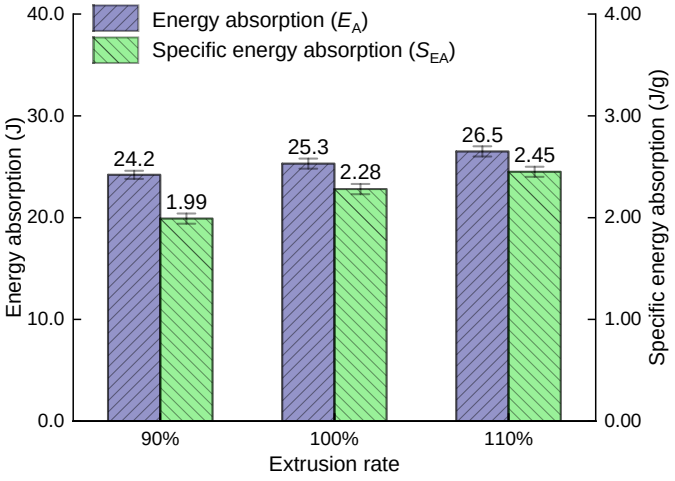

Fig. 4. Effect of extrusion rate on the energy absorption performance of gyroid infill structure

Effect of Extrusion Temperature on the Energy Absorption Performance of Gyroid Infill Structure

The compression energy absorption performance of three groups of gyroid infill specimens (three of each group) at 190, 210, and 230 °C extrusion temperatures is shown in Fig. 5. With increased extrusion temperature, the E_A value of the specimens increased, and the S_{EA} value increased. As the extrusion temperature increased, the temperature of the molten filament extruded from the extrusion head increased. More heat energy was emitted by the molten filament as it cooled from the viscous state to the glassy state, which promoted mutual diffusion and entanglement between adjacent layer filaments, resulting in an increase in the strength of the interlayer bonding of the adjacent layer filaments (Wang *et al*. 2023). Therefore, in the process of specimen compression, its overall structure is less prone to be damaged, so the E_A value is larger (Zhu *et al*. 2024). Because the change in extrusion temperature did not affect the mass of the specimen, the S_{EA} value of the specimen increased as the E_A value of the specimen increased. Thus, 230 °C was the optimised extrusion temperature to improve the energy absorption performance of the gyroid infill structure.

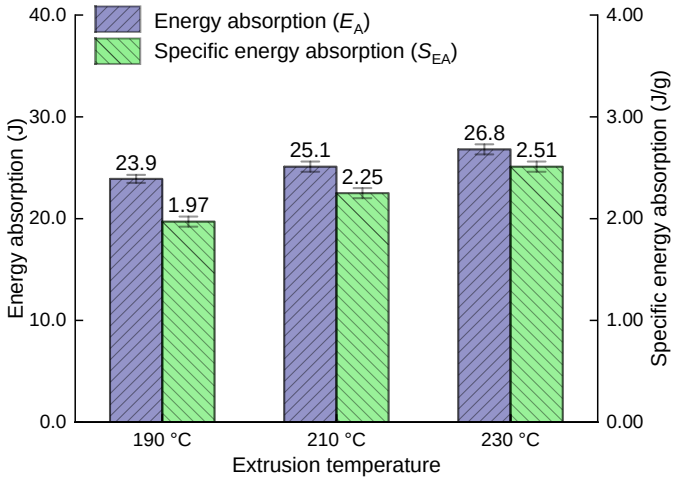

Fig. 5. Effect of extrusion temperature on the energy absorption performance of gyroid infill structure

Design and Rapid Prototyping

Reverse scanning

A classic representative of rosewood crafts (gourd ornament) was chosen as the design object. The gourd ornament, which means "fortune" and "wealth" in traditional Chinese culture, is hand-carved from rosewood and can be decorated in the home space or private car (Hu *et al*. 2024). The gourd ornament was scanned using a non-contact blue light 3D scanner (VTOP-300T, Visentech, Tianjin, China). Before scanning, the scanner was calibrated using a black and white grid calibration plate. Afterwards, a layer of developer was sprayed on the surface of the gourd ornament and marker dots were pasted to ensure that the blue light reflected on the surface of the gourd ornament is fully received by the CMOS camera, thereby ensuring the integrity of the point cloud model acquisition (Li and Hu 2023). When scanning, the gourd ornament was placed flat in the centre of the scanning platform, and the scanning angle was changed by rotating the scanning platform to obtain the point cloud model of the gourd ornament in any direction (Xia *et al*. 2024). At the same time, with the help of the positioning of the marking points, the point cloud model in different directions was spliced together, so as to obtain a complete point cloud model of the gourd ornament, and the reverse scanning live view of the gourd ornament is shown in Fig. 6.

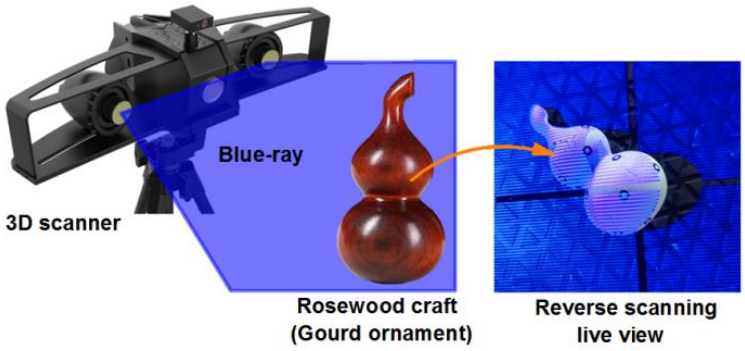

Fig. 6. Reverse scanning live view

Forward modelling

The scanned point cloud model (Fig. 7a) was imported into Geomagic software (Geomagic studio 12.0, NC, USA), and the point cloud model was encapsulated into a triangular sided model (Fig. 7b) by deleting the isolated and stray points outside the surface of the gourd ornament. Import the triangular sided model into Solidworks software and convert the triangular sided model into a surface model by using the feature recognition function (Fig. 7c). After that, a rectangular block was created as the base of the packaging liner, and the surface model of the gourd ornament was applied to cut the rectangular block, which was divided into two halves to obtain a solid model of the packaging liner that highly fits the surface of the gourd ornament (Fig. 7d). Finally, two sets of matching posts and holes were created on the packaging liner solid model for positioning and installation during packaging.

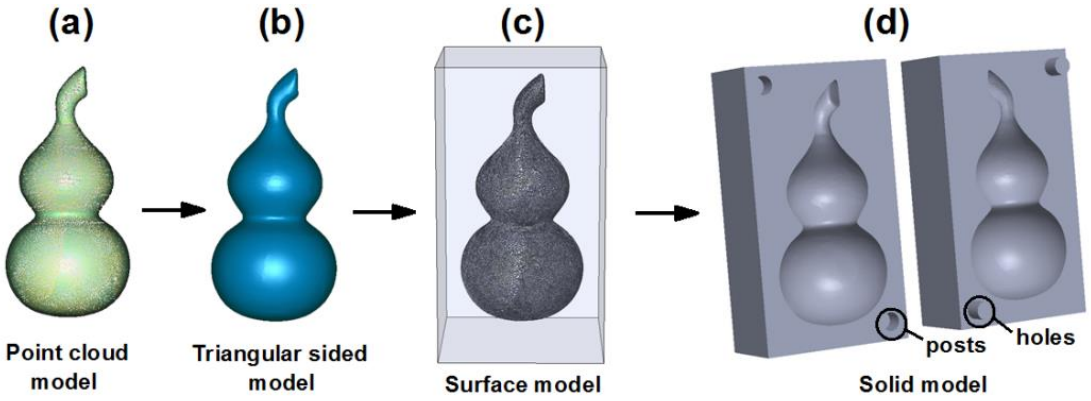

Fig. 7. Forward modelling process

Rapid prototyping

The STL model of the packaging liner was imported into Cura software for slicing, and the slicing parameters were set up with reference to the results of the compression test of the gyroid infill structure above, with the main parameters as follows: layer height of 0.2 mm, extrusion rate of 110%, and extrusion temperature of 230 °C. The sliced G-code file was imported into an FDM 3D printer to complete the 3D printing of the packaging liner rapid prototyping. The total printing time of the packaging liner was 50 min, and the total material consumption was 60 g. The printed packaging liner is shown in Fig. 8, and the assembled packaging liner is shown in Fig. 8.

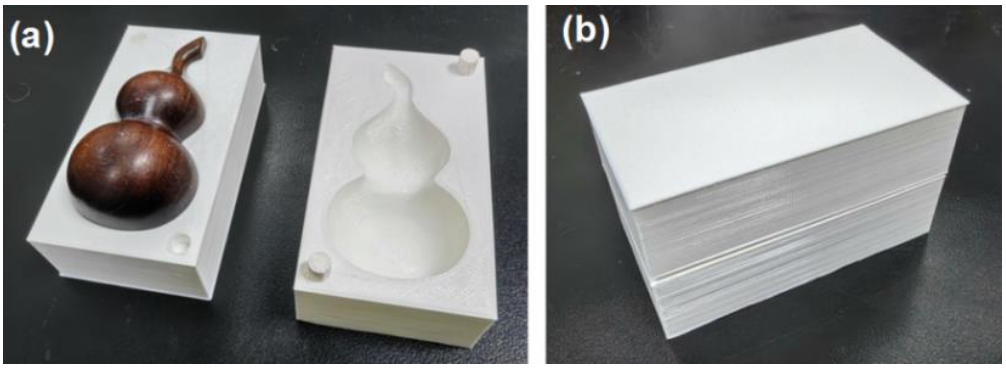

Fig. 8. 3D-printed packaging liner and assembled packaging liner

The 3D-printed packaging liner has a smooth outer surface with no printing defects, and its inner surface is highly adapted to the curved shape of the gourd ornament, making the overall structure easy to disassemble and assemble. Due to the strong resilience of the TPU filament and the strong energy-absorbing performance of the gyroid infill structure, the packaging liner can provide effective protection for the gourd ornament and provide guidance for the customized development of energy-absorbing packaging liners for other rosewood crafts.

CONCLUSIONS

1. With the decrease of layer height, the energy absorption (E_A) value of the gyroid infill structure increased, while the absorption of energy per unit mass (S_{EA}) value first increased and then decreased. With the increase of extrusion rate, the E_A value of the gyroid infill structure increased, and the S_{EA} value also increased. With the increase of extrusion temperature, the E_A value of the gyroid infill structure increased, and the S_{EA} value increased. The optimised printing parameters were as follows: layer height of 0.2 mm, extrusion rate of 110%, extrusion temperature of 230 °C.
2. The gourd ornament carved from rosewood was selected as the design object, and a packaging liner that highly fit the curved shape of the gourd ornament was designed through the process of reverse scanning and forward modelling. TPU filament was applied as the printing material to fabricate the packaging liner prototype by FDM 3D printing technology. The 3D-printed packaging liner developed based on gyroid infill structure and optimised printing parameters has strong energy-absorbing performance and can provide effective protection for the gourd ornament. In addition, further improving the design efficiency of the packaging liner and reducing the printing cost are the aspects that need to be improved in this study, and they are also the direction of our future research.

REFERENCES CITED

Chen, B.-R., Yu, X.-J., and Hu, W.-G. (2022). "Experimental and numerical studies on the cantilevered leg joint and its reinforced version commonly used in modern wood furniture," *BioResources* 17(3), 3952-3964. DOI: 10.15376/biores.17.3.3952-3964

Deng, J.-Z., Huang, N., and Yan, X.-X. (2023). "Effect of composite addition of antibacterial/photochromic/self-repairing microcapsules on the performance of coatings for medium-density fiberboard," *Coatings* 13(11), article 1880. DOI: 10.3390/coatings13111880

Ding, T.-T., Yan, X.-X., and Zhao, W.-T. (2022). "Effect of urea–formaldehyde resin–coated colour–change powder microcapsules on performance of waterborne coatings for wood surfaces," *Coatings* 12(9), article 1289. DOI: 10.3390/coatings12091289

Feng, X.-H., Yang, Z.-Z., Wang, S.-Q., and Wu, Z.-H. (2022). "The reinforcing effect of lignin-containing cellulose nanofibrils in the methacrylate composites produced by stereolithography," *Polymer Engineering and Science* 2022(9), 2968-2976. DOI: 10.1002/pen.26077

Han, Y., Yan, X.-X., and Zhao, W.-T. (2022). "Effect of thermochromic and photochromic microcapsules on the surface coating properties for metal substrates," *Coatings* 12(11), article 1642. DOI: 10.3390/coatings12111642

Hu, W.-G., Zhao, Y., Xu, W., and Liu, Y.-Q. (2024). "The influences of selected factors on bending moment capacity of case furniture joints," *Applied Sciences* 14(21), article 10044. DOI: 10.3390/app142110044

Huang, N., Yan, X.-X., and Zhao, W.-T. (2022). "Influence of photochromic microcapsules on properties of waterborne coating on wood and metal substrates," *Coatings* 12(11), article 1750. DOI: 10.3390/coatings12121857

Li, R.-R., Chen, J.-J., and Wang, X.-D. (2020). "Prediction of the color variation of moso bamboo during CO_2 laser thermal modification," *BioResources* 15(3), 5049-5057. DOI: 10.15376/biores.15.3.5049-5057

Li, S., and Hu, W.-G. (2023). "Study on mechanical strength of cantilever handrail joints for chair," *BioResources* 18(1), 209-219. DOI: 10.15376/biores.18.1.209-219

Li, W.-B., Yan, X.-X., and Zhao, W.-T. (2022). "Preparation of crystal violet lactone complex and its effect on discoloration of metal surface coating," *Polymers* 14(20), article 4443. DOI: 10.3390/polym14204443

Liu, Q., Gu, Y., Xu, W., Lu, T., Li, W., and Fan, H. (2021). "Compressive properties of green velvet material used in mattress bedding," *Applied Sciences* 11(23), article 11159. DOI: 10.3390/app112311159

Liu, Y., Hu, J., and Wu, Z.-H. (2020). "Fabrication of coatings with structural color on a wood surface," *Coatings* 10(1), article 32. DOI: 10.3390/coatings10010032

Mo, X.-F., Zhang, X.-H., Fang, L., and Zhang, Y. (2022). "Research progress of wood-based panels made of thermoplastics as wood adhesives," *Polymers* 14(1), article 98. DOI: 10.3390/polym14010098

Qi, Y.-Q., Sun, Y., Zhou, Z.-W., Huang, Y., Li, J.-X, and Liu, G.-Y. (2023). "Response surface optimization based on freeze-thaw cycle pretreatment of poplar wood dyeing effect," *Wood Research* 68(2), 293-305. DOI: 10.37763/wr.1336-4561/68.2.293305

Wang, L., Han, Y., and Yan, X.-X. (2022). "Effects of adding methods of fluorane microcapsules and shellac resin microcapsules on the preparation and properties of bifunctional waterborne coatings for basswood," *Polymers* 14(18), article 3919. DOI: 10.3390/polym14183919

Wang, Q., Feng, X.-H., and Liu, X.-Y. (2023). "Functionalization of nanocellulose using atom transfer radical polymerization and applications: A review," *Cellulose* 30, 8495-8537. DOI: 10.1007/s10570-023-05403-5

Xia, F., Wang, W., Zhang, J.-H., Yang, Y.-T., Wang, Q.-Y., and Liu, X.-Y. (2024). "Improving weed control through the synergy of waste wood-based panels pyrolysis liquid and rice husks: A sustainable strategy," *BioResources* 19(4), 7606-7618. DOI: 10.15376/biores.19.4.7606-7618

Yu, S.-L., and Wu, Z.-H. (2024). "Research on the influence mechanism of short video communication effect of furniture brand: Based on ELM model and regression analysis," *BioResources* 19(2), 3191-3207. DOI: 10.15376/biores.19.2.3191-3207

Yu, S.-L., Zheng, Q., Chen, T.-Y., Zhang, H.-L., and Chen, X.-R. (2023). "Consumer personality traits vs. their preferences for the characteristics of wood furniture products," *BioResources* 18(4), 7443-7459. DOI: 10.15376/biores.18.4.7443-7459

Zhu, Q., Yao, Q., Liu, J., Sun, J.-Z., and Wang, Q.-Q. (2020). "Emissions from the fused filament fabrication 3D printing with lignocellulose/polylactic acid filament," *BioResources* 15(4), 7560-7572. DOI: 10.15376/biores.15.4.7560-7572

Zhu, Y., Wang, Y., and Yan, X.-X. (2024). "Preparation of chitosan-coated *Toddalia asiatica* (L.) lam extract microcapsules and its effect on coating antibacterial properties," *Coatings* 14(8), article 942. DOI: 10.3390/coatings14080942

Article submitted: October 23, 2024; Peer review completed: November 15, 2024; Revised version received and accepted: November 17, 2024; Published: November 25, 2024.
DOI: 10.15376/biores.20.1.842-851